


The MOS Reduction Software - MRS

V. Bakış¹ 

¹Akdeniz University, Faculty of Science, Department of Space Sciences and Technologies, Kampus, Konyaaltı, Antalya, Turkey

Accepted: May 31, 2021. Revised: April 26, 2021. Received: March 24, 2021.

Abstract

An open source collection of computer programs has been developed and presented to the use of researchers to reduce the spectra taken with the multi-object spectrograph used as one of the focal plane instruments of RTT150 telescope in the TÜBİTAK National Observatory. Since the spectrograph has moving parts (i.e. grism, mask) and the pinholes on the mask are located at various locations with respect to dispersion axis, the spectra produced in the focal plane is exposed to some effects such as order tilts and wavelength shifts. A dedicated algorithm has been applied to determine and correct order tilts and wavelength shifts to extract the spectra from different pinholes, which can provide the basis of a pipeline reduction for the Observatory. The geometric distortion on the observed spectrum is found to be negligible which eliminates the need for complex algorithms for aperture extraction.

Key words: techniques: spectroscopic – techniques: image processing – Software

1 Introduction

The Multi Object Spectrographs (MOS) are one of the most important tools in observational astronomy. These devices make it possible to capture the spectra of many sources in the same field of view and to record them on the same CCD image. Therefore, one of the advantages that these devices offer to observers is the efficient use of telescope time. As an example, the MOS part of the Visible Multi-Object Spectrograph (VIMOS) installed at the European Southern Observatory's Very Large Telescope (VLT) in Chile allows observers to collect spectra of up to 1,000 stars or galaxies at a time (Le Fèvre et al. 2003). These devices are generally used in large telescopes (>6 m). There are a few examples in small and medium-size telescopes and TÜBİTAK National Observatory (TUG) is one such example with its 1.5 m diameter optical telescope, RTT150.

The MOS instrument in TUG is actually a device created with the modification of TUG Faint Object Spectrograph and Camera (TFOSC) instrument which is used as one of the focal plane instruments of the RTT150 telescope. TFOSC was build at Copenhagen University Observatory and it is the tenth of the FOSC series produced by the same institution. One of the most important advantages of the FOSC series is that it can be switched from imaging mode to spectroscopy mode in as little as one minute. In this way, the object to be observed by the spectrograph can be easily taken into the slit or pinhole located between the imaged area and the spectrograph elements. This feature allows the spectra of multiple sources to be taken simultaneously by using plates with many slits or pinholes following the general working principle of MOS devices.

With the commissioning of TUG's MOS instrument, many project calls were made. In order to get the desired outputs from the projects, an open-source reduction program dedicated to the MOS instrument data is needed. The article by Khamitov et al. (2020) in which they give a case study conducted using the TUG MOS instrument did not go beyond recommendations to the observers. Therefore, the need for an open source soft-

ware for observers to reduce their spectra taken with the MOS instrument has been a motivation for writing this article.

In the following sections, the data types that should be obtained before observations and that are used in data analysis are given (§2), the methodology followed in the MRS software is explained in its details (§3) and a conclusion with some advises is given in §4.

2 Data Requirements for MRS

Transactions such as observation preparation including preparing the mask figure for the region to be observed, computer aided manufacturing of the mask, adjusting the mask in the TFOSC filter slot etc. are successfully carried out by the TUG administration in cooperation with the project principle investigator (PI). Moreover, some observing techniques with the MOS are given given in TUG's web page. In the following, the data types and justifications of their usage needed for a reliable data reduction are provided.

Before giving details about the files needed for reduction with MRS, examining the work flow diagram of MRS (Fig. 1) could be useful for understanding the functioning of the processes in general terms. The code running the work flow in Fig. 1 is written in PYTHON programming language Van Rossum & Drake (2009), and the graphics are produced in several environments such as MATPLOTLIB, GNUPLOT (Williams et al. 2013) and SAOIMAGE/DS9 (Joye & Mandel 2003) environment depending on the task needed. SAOIMAGE/DS9 was used to show the fits files, aperture boundaries and the positions of the pinholes on the sky image, MATPLOTLIB for the interactive line definition task and GNUPLOT for the general graphic representation. The algorithm of the code shown in Fig. 1 is designed to present functions interactively to the user. The following frames and their features should have been obtained a-priori for a reliable data reduction.

- Bias (B) frames : Averaging several zero exposure bias frames reduces the impact of the readout noise which enables to estimate the correct bias level. Therefore, it is necessary to take several (>10 advised) Bias frames to properly represent the noise statistics and create master Bias frame. Master

* volkanbakis@akdeniz.edu.tr

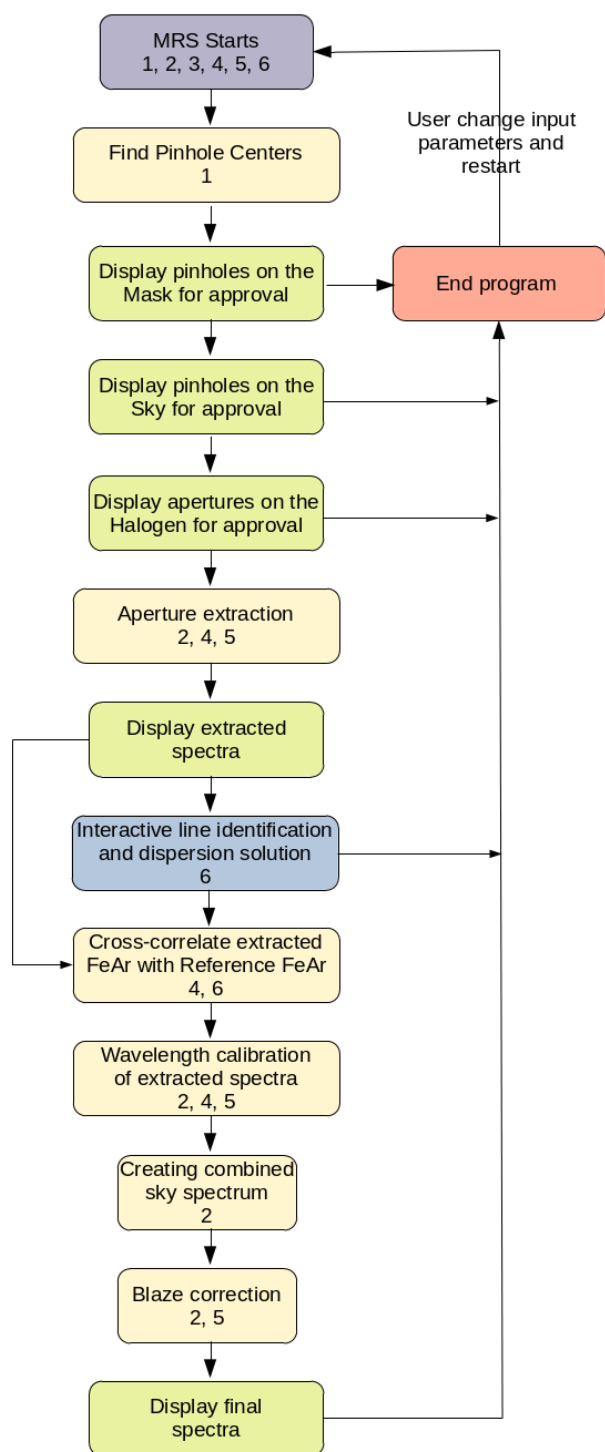


Figure 1. The work flow of MRS. The numbers in the boxes indicate the types of CCD images used for the relevant reduction step, which are 1. front illuminated mask image, 2. science spectrum taken with mask, 3. unfiltered image of the field, 4. FeAr lamp spectrum taken with mask, 5. Halogen lamp spectrum taken with mask and 6. FeAr slit spectrum.

Bias frame can be obtained by taking the mean value of the bias frames.

- Dark (D) frames : Since the present CCD camera (Andor iKon-L) attached to the TFOSC instrument can be cooled down to -90°C , the resulting dark current less than one electrons per pixel per hour (See [iKon-L specs](#)). As the dark currents increase with time, their exposure times should be equal to the exposure times of science frames. If they are not, it is possible to scale the dark frame by the ratio of exposure times, since dark current increases linearly with time and the linearity of the TFOSC CCD camera is given to be 1. While forming the master dark image, median combining is advised instead of mean value since at long exposures there may be cosmic rays which can be detected and removed by median master dark frame.
- PRNU (Photoresponse non-uniformity) image: This must be provided by TUG as it can be obtained by detaching the CCD camera. This image must be provided by the TUG as it can be obtained by separating the CCD camera from the TFOSC unit. After obtaining the PRNU image, the CCD frames (S) of mask, science (object spectrum and unfiltered image of the region), FeAr and halogen lamp are made ready for reduction by MRS by applying $(S - D)/(PRNU - B)$ arithmetic. The data preparation process up to this stage is left to the user using existing data reduction package(s) such as IRAF ([Tody 1986](#)).
- Mask definition file (MDF): This is a FITS binary file created by exposing the mask which is illuminated in the front. A reliable determination of the coordinates of the pinholes is only possible by analyzing this image. Otherwise, these coordinates can be determined using less reliable methods such as estimating the y-coordinates from the average position of the spectral order on the CCD frame and the x-coordinate from the wavelength shift of the spectral order.
- Halogen (F) lamp spectra: In the absence of PRNU frame, this frame is required to correct the pixel-to-pixel variations along the CCD frame. They can also be used for the correction of the blaze function and the removal of the fringes. At least 10 halogen lamp spectra taken with the mask are suggested.
- FeAr lamp spectra taken with mask: Mask spectrum of FeAr lamp is used for wavelength calibration of the extracted spectra. Since the dispersion of the spectrum obtained by using Grism 15 is in the range of $1.9\text{--}3.0 \text{ \AA pixel}^{-1}$, normally a single FeAr lamp spectrum taken with the mask and with an ideal exposure time is enough.
- FeAr lamp slit spectrum taken without mask: Slit spectrum of FeAr lamp is used to calibrate the shifts of the wavelengths due to positional change of the pinholes.
- CCD image (preferably unfiltered) of the region: This frame is used for approving the location of the pinholes and for selection of the science objects or sky regions. This image has to be taken just before the exposure for the spectrum.
- Science spectrum (S): Spectrum of the field taken with the mask which is properly aligned to get the spectra of the program objects within correct pinholes. The exposure time of the spectrum should be arranged according to Exposure Time vs. Signal-to-Noise Ratio (S/N) table prepared for different magnitude and spectral type stars. For objects fainter than 16 magnitude, more than 1800 s exposure time is advised (See [MOS manual](#)).

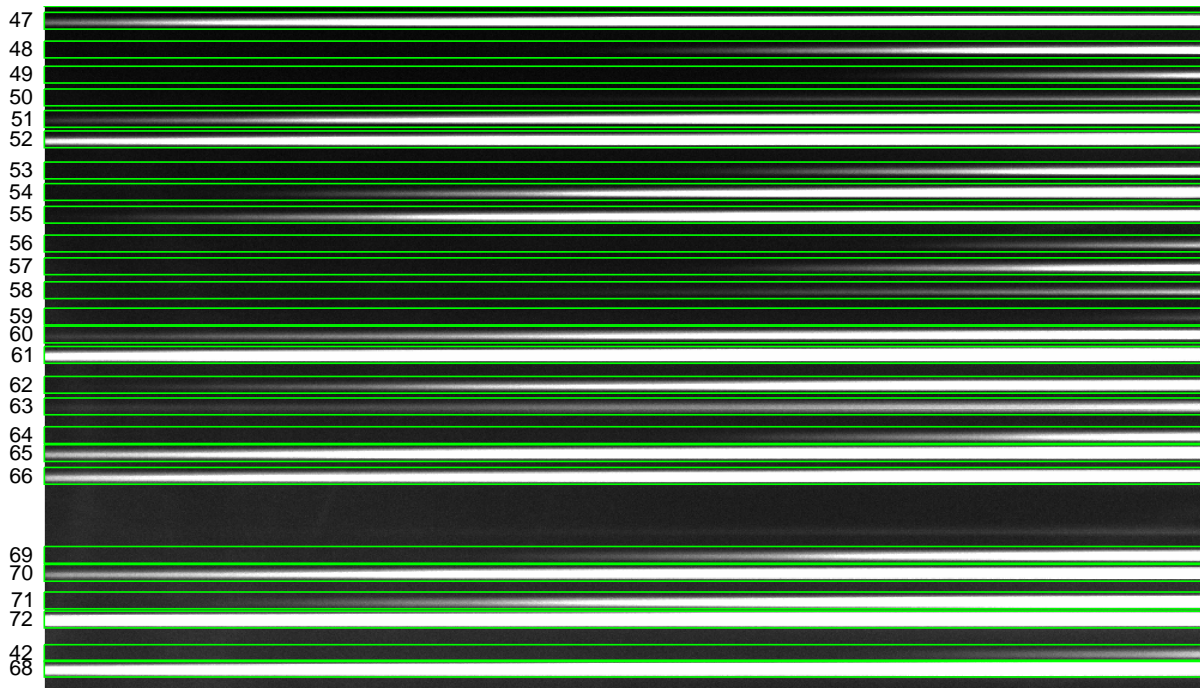


Figure 3. Part of the halogen lamp spectra for some pinholes (from 43 to 66) and rectangular (green) aperture extraction regions with adjustable width and specific numbers (on the left edge) for each pinhole.

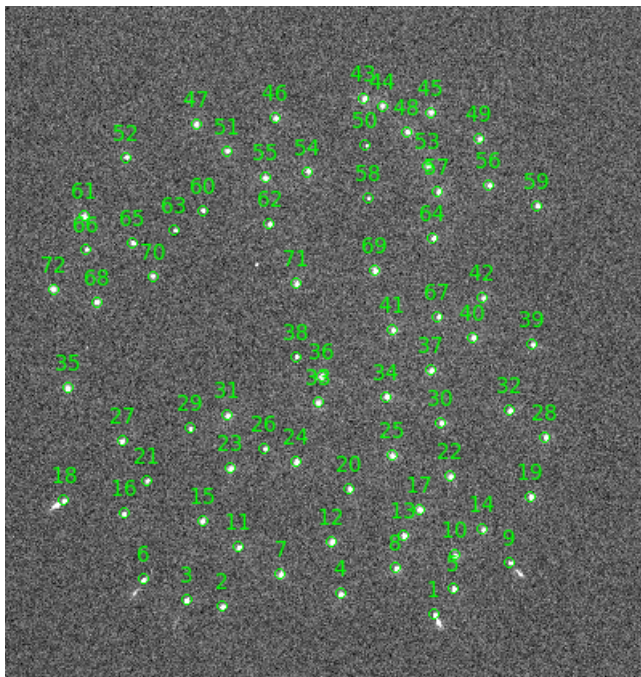


Figure 2. Pinholes in an example MDF.

3 Reduction Methodology

The MRS workflow consists of the following main stages, shown in Fig. 1:

- a. Locating the pinholes in the mask definition file (MDF),

- b. Extracting apertures for Halogen, FeAr, Calibration and Science frames,
- c. Line identification for FeAr lines and dispersion solution,
- d. Cross-correlation of the FeAr frames with the Calibration frames to determine the wavelength shifts due to different pinhole locations,
- e. Creating the combined sky spectrum,
- f. Correction of the Blaze function by dividing Science spectra by Halogen spectra.

3.1 Determining locations of the pinholes

Pinholes act like a stellar source on the MDF (see Fig. 2). Therefore, their physical locations could be extracted using the Source Extractor (SEXTRACTOR) (Bertin & Arnouts 2010) code. This code gives us an advantage in distinguishing point and diffuse sources. As can be seen from the figure, besides some point sources, there are some diffuse sources due to the optical distortions in the TFOSC (see below aperture number 1, 6, 18 and 9). By default, the MRS is set so that the SEXTRACTOR can detect pinholes in the MDF. However, the user can change these parameters in the coordinate ascii files, depending on the situation. Especially if the SEXTRACTOR code cannot calculate the center coordinates of the resources correctly, which is possible since the pinholes are not perfectly created (see Khamitov et al. 2020), it will cause the aperture extraction regions shown in the Fig. 3 to shift and thus cause incorrect aperture extraction. In this case, the importance of the program's option for user approval at every step becomes apparent. The user can set the required parameters to terminate the program and start over at any stage. After the aperture coordinates are determined, the user is presented an image of the observed area with the pinholes on top of each other. At

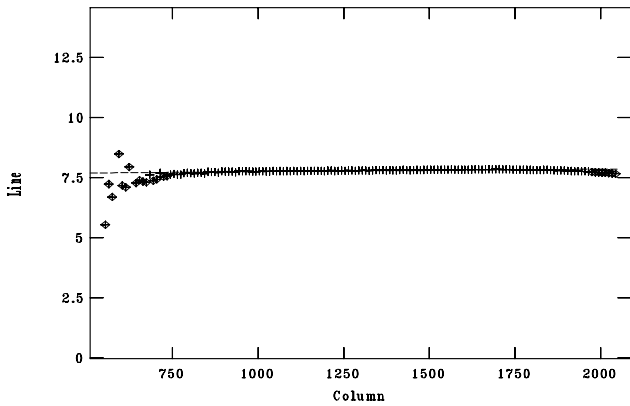


Figure 4. Distribution of aperture maximum (pluses) along the spectral order for aperture number 49 of halogen lamp spectrum. Outstanding points (diamonds) from the aperture function are visible on the edges.

this stage, the pinhole numbers to be used for source(s) and sky can be noted.

3.2 Aperture extraction

Depending on the orientation of the grism in the filter wheel of the TFOSC, the orders can make a slope on the CCD frame. This orientation should be determined during the approval of aperture zones and corrected by entering the appropriate angle in the MRS configuration file. After the orientation of the orders is corrected, the aperture tracing along the dispersion direction as shown in Fig. 4. Each point in the figure represents the coordinates of the relevant aperture maximum value along the CCD column. It is clear that once the orientation of the order is set correctly the deviation of the aperture maximum along the vertical axis (line) is less than a pixel meaning that summing column pixel values in ADU ($P_{x,\lambda}$) along the aperture box vertical axis (x) is an appropriate way of extracting the spectrum (S_λ). Therefore, the aperture extraction algorithm is performed as given by Eq. 1:

$$S_\lambda = \sum_{x=1}^{12} P_{x,\lambda} \quad (1)$$

where the size of the axis (x) which is perpendicular to the dispersion axis (λ) is taken to be 14 by default and can be altered by the user.

3.3 Dispersion solution and calibrating the shifted FeAr spectra

The fact that the pinholes on the mask are at different positions along the dispersion axis causes it to make a different angle with the grism normal axis, thus causing the wavelength shift according to Eq. 2:

$$\sin(\alpha) + \sin(\beta) = mk\lambda \quad (2)$$

where α and β are incident and diffracted light angles, m is order number, k is grism groove density and λ is wavelength. As k is constant for a certain grism, the location of wavelength λ changes as the incident light angle (α) changes for a specific spectral order number m . However, since the properties of the grism are preserved, the dispersion solution is also preserved.

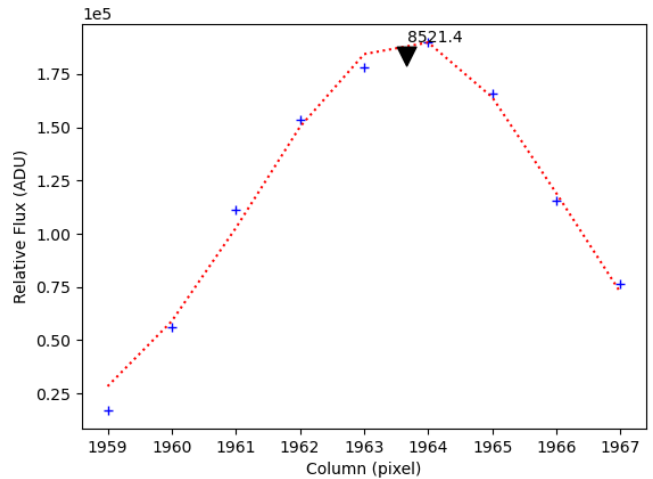
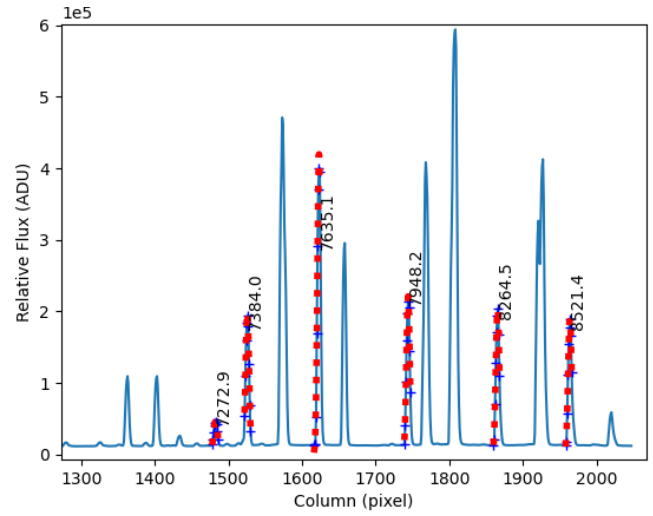


Figure 5. Top panel: A view from line identification window. Bottom panel: A view from gaussian fit to a selected emission line center at 8521.4Å.

Thus, if a dispersion solution is obtained for a selected pinhole, it can be used for other pinholes once their spatial shifts are known.

Thus, if it has not been done before, the dispersion solution must first be made with line identification. This step is the next step after displaying the extracted spectrum as shown in Fig. 5 top panel, which helps the user to select the most suitable pinhole for line identification. Because the line identification to be made for this pinhole will be a reference for other spectra. Gaussian profiles are fitted to the selected spectral lines interactively during the line identification procedure. Thus, the user only needs to enter an approximate pixel coordinate value for the relevant line (see Fig. 5 bottom panel).

At the end of the line identification process, the coefficients of the quadratic polynomial dispersion function determined for the grism 15 are given in a table as in Table 1.

The shifts of all FeAr spectra from different pinholes are determined by cross correlating them with the the reference spectrum. For this purpose, the DCF3 (discrete correlation function) algorithm, which is used by Robertson et al. (2015) in their study, is adopted in MRS. For some pinholes, cross-correlation function (CCF) shows many peaks with amplitudes

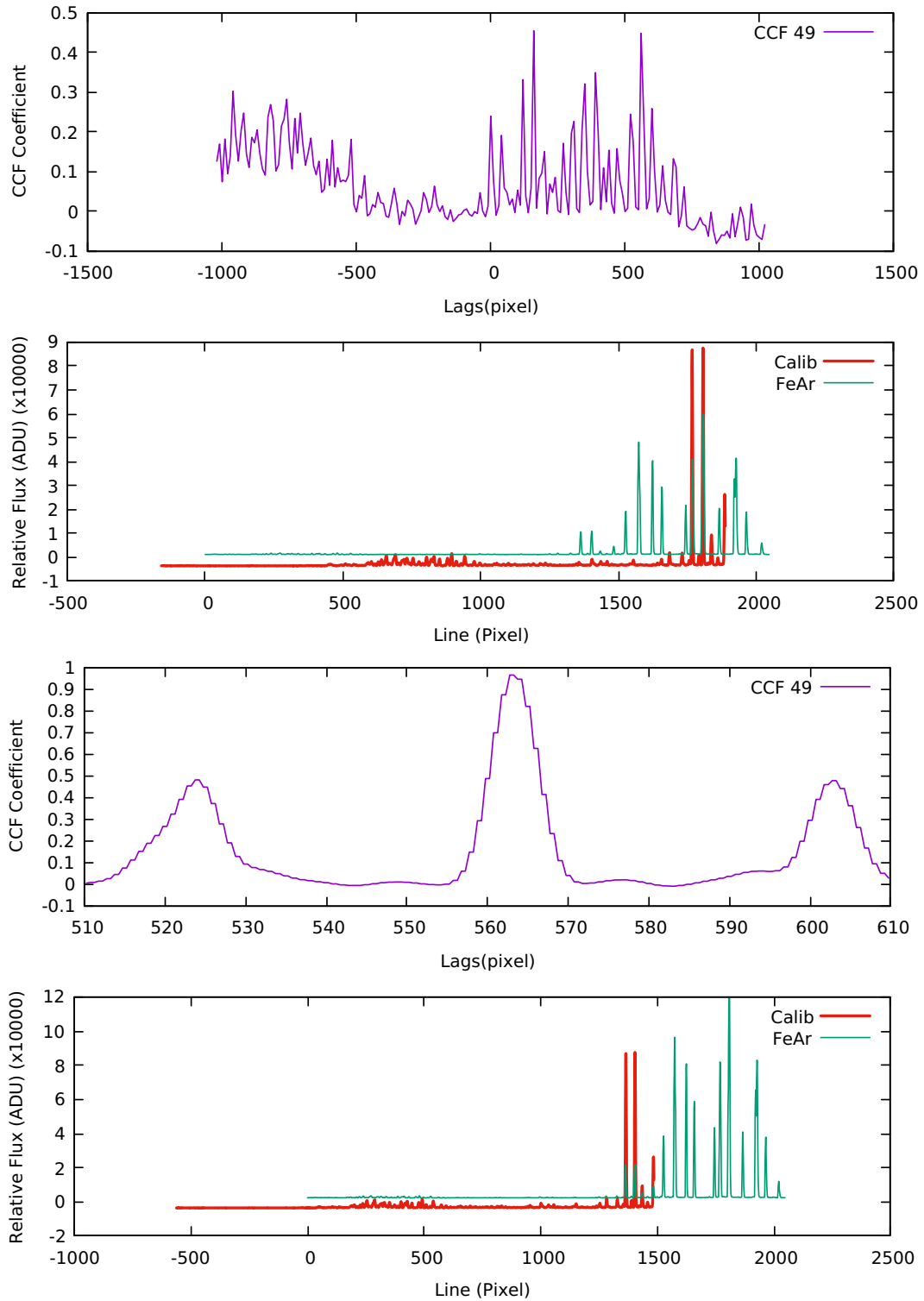


Figure 6. Top two panels: Similar amplitude peaks (upper panel) in the CCF. Reference FeAr spectrum taken with slit and FeAr spectrum taken with mask are shown in green and red (bottom panel), respectively. **Bottom two panels:** Corrected shift of FeAr spectrum with respect to reference spectrum for pinhole #49.

close to each other (see Fig. 6, top two panels), and since the code selects the highest peak as the best matching shift, the true shift may not be detected. For these cases, another code is developed in the MRS environment to correct the shift by selecting the appropriate peak in the CCF function, which can be

run separately outside of the MRS. The correct shift and CCF for aperture #49 is shown in Fig. 6 (bottom two panels).

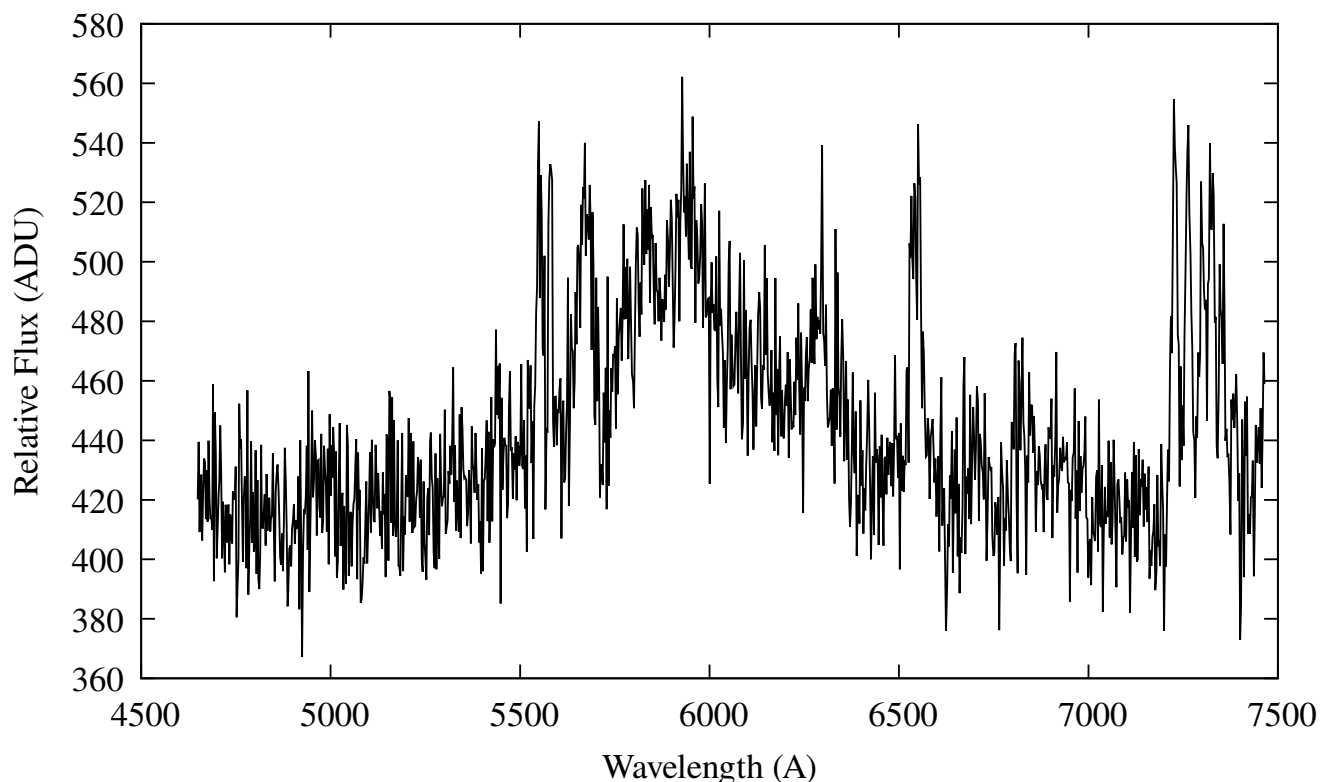


Figure 7. Sky spectrum created by combining several sky spectra from different pinholes.

Table 1. Dispersion function ($y = a_0 + a_1x + a_2x^2 + a_3x^3$) coefficients for grism 15.

a_0	a_1	a_2	a_3
1.41185	0.000312139	-2.46627e-08	5.05286e-13

3.4 Combined sky spectrum

If the radiation from the sky (sky brightness and emissions at certain wavelengths) is desired to be avoided, they must be excluded from the science spectrum. Since the spectrum of the sky depends on the wavelength, this cannot be done by pixel-to-pixel subtraction alone, and prior wavelength calibration is a must. For this reason, a master sky spectrum is first created by taking the median of the spectra of the pinholes selected for the sky regions. Sigma clipping algorithm is applied in calculating the sky median. That is, values that are 2σ greater or less than the sky median value are excluded. Therefore, it is recommended to combine a minimum of 5 (larger the number, the more reliable it will be) sky region spectrum to obtain a statistically reliable master sky spectrum.

Regarding the wavelength calibration, it should not be forgotten that pinholes with different horizontal positions (in the dispersion axis) also have different wavelength ranges. Therefore, in order to combine more than one spectrum, sky fluxes of the same wavelength of spectra must overlap. This requires careful shifting in the dispersion axis for each sky spectrum while creating a master sky spectrum, which is done in MRS.

In Fig. 7, a master sky spectrum created from 6 sky images is shown as an example.

3.5 Blaze function correction

In general, it is recommended to leave the blaze function in the spectrum as it is (See [DOECSLIT manual](#)). The main reason for this is that the arc lamp (halogen, tungsten, led or combined) chosen to create the flat image is wavelength dependent and the flat image cannot fully represent the blaze function since it includes the shape of the flat field spectrum and the grism blaze function. However, the flat spectrum can be used to correct for fringe effects seen in the spectrum. These **fringes** are due to the coating of the glass surface in front of the CCD chip to protect it from external influences. In addition, this effect is wavelength dependent and variable at different amplitudes on the CCD surface. The halogen lamp spectrum for each pinhole is created in MRS and the division of science spectrum with the halogen lamp spectrum is performed as the program outputs. In Fig. 8, flat field corrected science spectrum is shown of a star (GAIA source 2007374122533029248, $m_g = 16.^m2$) with the science spectrum uncorrected.

4 Conclusion

The MOS instrument has brought an important capability to the RTT150 telescope. In order to provide the most efficient output from the scientific projects to be carried out using this instrument, an open source code reduction program, which is open to the access of all researchers, easy to use, and whose scientific basis is clearly stated, was needed. For this purpose,

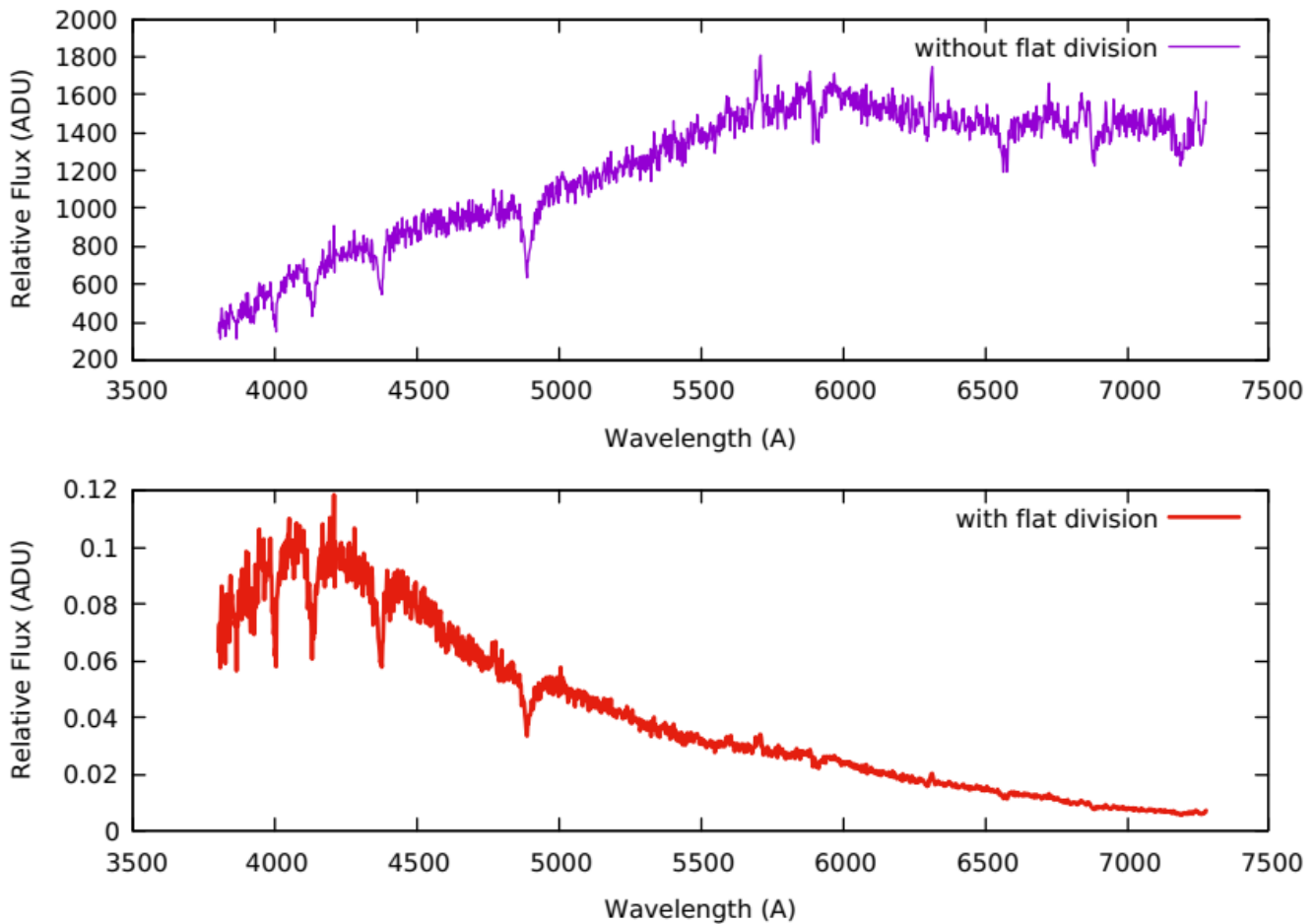


Figure 8. Final spectrum of a $m_g = 16^m2$ star (GAIA source 2007374122533029248) with and without flat field correction.

a set of computer reduction programs called MRS was written to reduce the MOS spectra obtained with TFOSC by using graphical interfaces such as GNUPLOT and DS9 together with the powerful libraries of the PYTHON programming language. The code MRS will be available online to all MOS users under GNU General Public License v3.0.

Flat field division of the aperture extracted and wavelength calibrated spectrum must be done very carefully as this process may cause unwanted effects on the reduced spectrum. A flux standard star observation and flux calibration of the program stars are strongly advised. Since pinholes on the mask are not created perfectly and there may be some micro-scale roughness on the edges, it is very important to align the pinhole to exactly center the science objects, otherwise it may cause all observational data to be wasted since it will cause a wrong flux calibration.

In the near future, it is planned to add the optimal spectrum extraction algorithm introduced by Horne (1986) study as an alternative spectrum extraction procedure to the current (default) one.

Acknowledgement

Special thanks to Hicran BAKIŞ, Aytap SEZER and Günay PAYLI for making their MOS data available during the development of MRS.

References

- Bertin E., Arnouts S., 2010, SExtractor: Source Extractor (ascl:1010.064)
- Horne K., 1986, *PASP*, 98, 609
- Joye W. A., Mandel E., 2003, in Payne H. E., Jędrzejewski R. I., Hook R. N., eds, *Astronomical Society of the Pacific Conference Series Vol. 295, Astronomical Data Analysis Software and Systems XII*. p. 489
- Khamitov I. M., Bikmaev I. F., Burenin R. A., Glushkov M. V., Melnikov S. S., Lyapin A. R., 2020, *Astronomy Letters*, 46, 1
- Le Fèvre O., et al., 2003, in Iye M., Moorwood A. F. M., eds, *Society of Photo-Optical Instrumentation Engineers (SPIE) Conference Series Vol. 4841, Instrument Design and Performance for Optical/Infrared Ground-based Telescopes*. pp 1670–1681, doi:10.1117/12.460959
- Robertson D. R. S., Gallo L. C., Zoghbi A., Fabian A. C., 2015, *MNRAS*, 453, 3455
- Tody D., 1986, in Crawford D. L., ed., *Society of Photo-Optical Instrumentation Engineers (SPIE) Conference Series Vol. 627, Instrumentation in astronomy VI*. p. 733, doi:10.1117/12.968154
- Van Rossum G., Drake F. L., 2009, *Python 3 Reference Manual*. CreateSpace, Scotts Valley, CA
- Williams T., Kelley C., many others 2013, *Gnuplot 5.4: an interactive plotting program*, <http://gnuplot.sourceforge.net/>

Access:

M21-0103: *Turkish J.A&A* — Vol.2, Issue 1.